

Copper pyrites CuS_2 and CuSe_2 as anion conductors

Hiroaki Ueda, Minoru Nohara, Koichi Kitazawa, and Hidenori Takagi*

Department of Applied Chemistry and Department of Advanced Materials Science, University of Tokyo, 7-3-1 Hongo, Bunkyo-ku, Tokyo 113-8656, Japan

Atsushi Fujimori and Takashi Mizokawa

Department of Complexity Science and Engineering, University of Tokyo, 7-3-1 Hongo, Bunkyo-ku, Tokyo 113-8656, Japan

Takehiko Yagi

Institute for Solid State Physics, University of Tokyo, 5-1-5 Kashiwanoha, Kashiwa-shi, Chiba 277-8581, Japan

(Received 4 August 2001; published 27 March 2002)

CuS_2 and CuSe_2 with pyrite structures were systematically studied by transport, magnetization, and specific-heat measurements. In remarkable contrast to other 3d transition-metal pyrites, a clear indication of strong electron correlations was absent in the electronic properties of Cu pyrites. We interpret this as a consequence of the dominant chalcogen p character rather than copper d character at the Fermi level. Photoemission results indeed support this picture, indicating that the Cu is predominantly monovalent. We therefore conclude that Cu pyrites, CuS_2 and CuSe_2 , can be viewed as anion conductors.

DOI: 10.1103/PhysRevB.65.155104

PACS number(s): 71.20.Ps, 72.80.Ga, 74.70.Ad, 79.60.Bm

I. INTRODUCTION

Among the 3d transition-metal dichalcogenides MX_2 , those with $M = \text{Fe}, \text{Co}, \text{Ni}, \text{Cu},$ and Zn , and $X = \text{S}$ and Se , are known to crystallize in the so-called pyrite structure.¹ The pyrite structure contains interpenetrating face-centered-cubic arrays of metal cations and anion dimers, as in the rocksalt structure (Fig. 1). Each cation is in the center of an anion octahedron, and each anion atom has a tetrahedral coordination consisting of one anion atom and three cations. Because of the strong p - p hybridization within the chalcogen anion dimer, each anion dimer can accommodate two electrons in its bonding $p\sigma$ orbital but not in the antibonding $p\sigma^*$ orbital, serving as divalent X_2^{2-} in a naive ionic picture. Transition-metal cations, therefore, are formally divalent, M^{2+} , and take a low spin electronic configuration $t_{2g}^6 e_g^n$ ($n = 0, 1, 2, 3,$ and 4 for $M = \text{Fe}, \text{Co}, \text{Ni}, \text{Cu},$ and Zn , respectively).

These pyrites have been attracting considerable interest for many decades, because of their rich variety of electronic and magnetic properties. A drastic variation of the ground state with the number of e_g electrons per unit formula can be seen in the sulfides. FeS_2 without an e_g electron is a non-magnetic (band) insulator. While CoS_2 with one e_g electron is an itinerant ferromagnet, NiS_2 with two e_g electrons is an antiferromagnetic (Mott) insulator. The Ni pyrite, showing a metal-insulator transition caused by pressure or chemical substitution, has been viewed as a model system of correlation-driven metal-insulator transitions.² CuS_2 , which was supposed to have three e_g electrons, was reported to be a metal.³⁻⁵ ZnS_2 , with four e_g electrons, is a diamagnetic insulator. The wide varieties of magnetic phases in these sulfides indicate a vital role of electron correlations in the narrow transition-metal 3d band. On the other hand, the selenide compounds have been known as a paramagnetic metal except when the metal cation is Fe^{2+} (e_g^0) and Zn^{2+} (e_g^4),

consistent with the prediction of band theory. This drastic change from sulfides to selenides very likely implies that the magnetic phases in the sulfides are marginally achieved.

Generally speaking, as the cation goes from light to heavy transition metals, the on-site d - d Coulomb repulsion U becomes larger, and electron correlations become more important. On the other hand, simultaneously, the charge-transfer energy Δ from the anion p orbitals to the d orbitals decreases. Not only the on-site d - d Coulomb repulsion but also the charge transfer from the chalcogen p orbitals to the metal d orbitals very likely play an important role in the physics of those pyrites with heavy 3d transition metals, particularly for Ni and Cu. Band-structure calculations on the pyrites indeed showed that the broad band of chalcogen p states is located very close in energy to the metal d states.⁶ In FeS_2 and CoS_2 , the e_g band seems to lie right above the top of the occupied p band. On the other hand, in ZnS_2 the p band lies right above the e_g band. NiS_2 and CuS_2 are located between CoS_2 and ZnS_2 , where the subtle interplay between the cation $d(e_g)$ orbitals and the anion p orbitals should be most pronounced. In accord with this, because of the small Δ ($< U$), NiS_2 is classified as a charge-transfer insulator. In

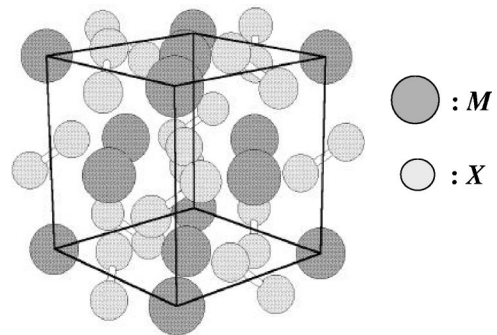


FIG. 1. Crystal structure of pyrite MX_2 [M : transition-metal elements (black circle); X : chalcogen elements (gray circle)].

charge-transfer insulators, the top of the occupied p band is located between the occupied lower Hubbard band and the unoccupied upper Hubbard band, and the lowest charge excitation is the charge transfer from the occupied p level to the unoccupied d level.

Even larger U and smaller Δ than NiS_2 are anticipated for CuS_2 . Compared with the other pyrites, however, copper pyrites have not been studied in detail because of their difficulty in synthesis. Copper pyrites were first synthesized under a high pressure above 3 GPa.^{7,3} Although the detailed temperature dependence was not examined, the resistivity of copper pyrites was reported to show a metallic behavior. Both the sulfide and selenide were reported to experience a superconducting transition at a low temperature, with $T_c = 1.5$ and 2.4 K, respectively.^{3,4} Among the pyrites known so far, copper pyrites are the only superconducting compounds.

While CuS_2 was reported to show a weakly temperature-dependent paramagnetism, the magnetic properties of CuSe_2 proved controversial. Depending on the sample preparation condition, CuSe_2 was reported to show a weak ferromagnetism below 31 K.⁸ These weakly ferromagnetic samples, as well as the paramagnetic samples, showed superconductivity. The possible coexistence of weak ferromagnetism and superconductivity in CuSe_2 is an attractive subject to pursue.

The importance of electron correlation and the effects of p - d hybridization on copper pyrites, as well as the coexistence of weak ferromagnetism and superconductivity in CuSe_2 , motivated us to investigate copper pyrites. We prepared single crystals of CuS_2 and CuSe_2 under high pressure, and explored the electronic states of seemingly p - d metals, by systematic measurements of transport, magnetization, specific heat, and photoemission spectroscopy (PES). Remarkably, we did not find a noticeable transport and specific heat signature of strong electron correlations, normally observed in strongly correlated transition-metal compounds. We interpret this observation as due to the predominant p character at the Fermi level, and propose that the electronic structure can be better represented by $\text{Cu}^+(X_2)^-$ with one hole in the anion p band as charge carriers. We were indeed able to verify this picture by PES measurements. In this regard, copper pyrites may be viewed as anion “ p metals.”

II. EXPERIMENTAL METHOD

All samples used in this study were prepared under high pressure, generated by a cubic anvil-type press.⁹ A boron nitride crucible was used as a sample container. Single crystals of CuS_2 and CuSe_2 were grown at 5 GPa with 1:1 mixtures of CuS/S and CuSe/Se as starting materials. The mixtures were slowly cooled from about 600 to 400 °C in 3 h. All the samples were characterized by powder x-ray diffraction, which revealed the absence of secondary phases within our experimental resolution. Single crystals with a typical dimension of $1.0 \times 1.0 \times 0.5 \text{ mm}^3$ were obtained from the solidified melt. The electrical resistivity was measured by a conventional four-probe technique with a low-frequency resistance bridge. The Hall coefficient measurements were conducted by rotating the sample in a magnetic field of 1.4 T. A superconducting quantum interference device magnetome-

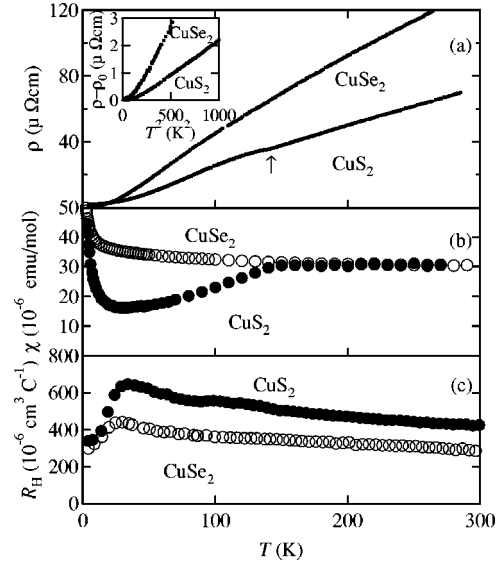


FIG. 2. (a) Temperature-dependent resistivity of CuS_2 and CuSe_2 single crystals. The arrow indicates an anomaly of CuS_2 . The inset shows $(\rho - \rho_0)$ vs T^2 plots at low temperatures, where ρ_0 is the residual resistivity. (b) Temperature-dependent Hall coefficient of CuS_2 and CuSe_2 single crystals. (c) Temperature-dependent magnetic susceptibility of CuS_2 and CuSe_2 single crystals, measured at 1000 G.

ter was used for the magnetization measurements. The specific-heat measurements were performed by a relaxation-type calorimeter. To probe the electronic structure directly, ultraviolet photoemission spectroscopy (UPS) measurements at room temperature were carried out, using a spectrometer equipped with a helium discharge lamp (He I: $h\nu = 21.2 \text{ eV}$; He II: $h\nu = 40.8 \text{ eV}$). Clean surfaces were obtained by scraping the sample *in situ* with a diamond file. The energy resolution including the thermal broadening was $\approx 0.1 \text{ eV}$.

III. RESULTS

The electrical resistivity data $\rho(T)$ of single crystals of CuS_2 and CuSe_2 , displayed in Fig. 2(a), show a metallic behavior, which is consistent with the band-structure calculation. For both compounds, the temperature dependence is consistent with those published previously,⁵ though the absolute values are smaller by a factor of ~ 2 . An anomaly is observed in CuS_2 at about $T^* \approx 150 \text{ K}$ [indicated by an arrow in Fig. 2(a)], in agreement with a previous report.⁵

Hall coefficients R_H , shown in Fig. 2(b), are positive and weakly temperature dependent, both for CuS_2 and CuSe_2 . The positive sign of R_H implies that the charge carriers are predominantly hole-like. This result disagrees with the previous report, in which R_H was negative.⁵ We do not have any plausible explanation for this discrepancy. The carrier density, calculated from the magnitude at 300 K, is about one hole per unit formula. A noticeable decrease can be seen below 30 K, which may be ascribed to the effect of the complicated Fermi-surface geometry¹⁰ and the momentum-dependent scattering. These results are consistent with the naive band picture.

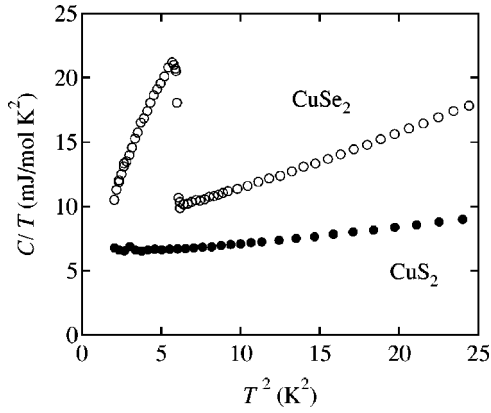


FIG. 3. Temperature-dependent specific heat $C(T)$, plotted C/T vs T^2 , for CuS_2 and CuSe_2 .

The magnetic susceptibility $\chi(T)$ of the Cu pyrites is shown in Fig. 2(c). Both CuS_2 and CuSe_2 show weakly temperature-dependent paramagnetism. A trace of a Curie-like contribution is seen at low temperatures, which very likely originates from a small amount of magnetic impurities. In CuS_2 , a clear anomaly is observed at $T^* \approx 150$ K, where a kink is observed in $\rho(T)$, and a pronounced decrease of $\chi(T)$ is observed below T^* , as reported before.¹¹ The $\chi(T)$ of CuSe_2 is almost temperature independent, and no anomaly can be seen. Previous work reported the presence of weak ferromagnetism in CuSe_2 , which depends on the sample preparation condition.⁸ However, we did not find any trace of weak ferromagnetism over a wide variety of samples, prepared under different conditions, including those employed in previous work. By subtracting the Curie term and the core diamagnetism, $\chi_{\text{core}}(\text{Cu}^{2+}) = -1.1 \times 10^{-5}$ emu/mol, $\chi_{\text{core}}(\text{S}_2^{2-}) = -4.4 \times 10^{-5}$ emu/mol, and $\chi_{\text{core}}(\text{Se}_2^{2-}) = -6.6 \times 10^{-5}$ emu/mol,¹² we estimated the paramagnetic contribution χ_{para} at low temperatures, which is very likely dominated by the Pauli paramagnetism of conduction electrons: $\chi_{\text{para}}(\text{CuS}_2) = 6.4 \times 10^{-5}$ emu/mol and $\chi_{\text{para}}(\text{CuSe}_2) = 11.0 \times 10^{-5}$ emu/mol.

Previous electron microscopy studies revealed that the anomaly at $T^* \approx 150$ K in CuS_2 is accompanied with a structural phase transition;^{13,14} therefore, the formation of a charge density wave (CDW) was suggested as the origin of this anomaly.⁸ However, we believe that the transition at T^* is not a CDW but is essentially structural in origin. This is because no anomaly is detected in R_H around T^* , in remarkable contrast with those observed in CDW systems such as NbSe_2 and TaSe_2 .¹⁵ R_H directly measures the charge carriers around the Fermi surface and, hence, is one of the most sensitive probes for the CDW formation. We suspect that the above-mentioned decrease of the magnetic susceptibility below T^* may originate from a Van Vleck contribution.

The results of specific-heat measurements are summarized in Fig. 3. Except for the temperature range below the superconducting transition in CuSe_2 , the low-temperature specific heat is well described by $C(T) = \gamma T + \beta T^3$. The Debye temperatures obtained from the β values are $\theta_{\text{Dth}}(\text{CuS}_2) = 280$ K and $\theta_{\text{Dth}}(\text{CuSe}_2) = 170$ K. The electronic specific-heat coefficients γ obtained are $\gamma(\text{CuS}_2) = 6.18$ mJ mol⁻¹

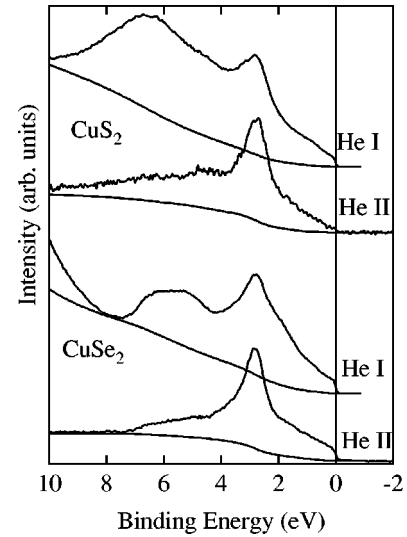


FIG. 4. UPS spectra of CuS_2 and CuSe_2 , with two different incident phonon energies, 21.2 eV (He I) and 40.8 eV (He II). Note the He II spectra mainly reflects the 3d contribution.

K^{-2} and $\gamma(\text{CuSe}_2) = 7.37$ mJ mol⁻¹ K⁻².

A clear specific-heat jump associated with superconducting transition is observed in CuSe_2 at $T_c = 2.47$ K, which is in agreement with that reported previously. The ratio of the specific-heat jump at T_c in CuSe_2 relative to the electronic specific heat is $\Delta C/\gamma T_c = 1.50$. This value is close to the value of Bardeen-Cooper-Schrieffer (BCS) theory 1.43, and suggests that CuSe_2 is a weak-coupling BCS superconductor.

Figure 4 shows the photoemission spectra (He I and He II) of CuS_2 and CuSe_2 , which are normalized to the Cu 3d t_{2g} peak height. It is known that σ_p/σ_d decreases with photon energy, where σ_p and σ_d are the atomic photoionization cross sections of the chalcogen p and Cu 3d orbitals, respectively.¹⁶ As a result, the He I ($h\nu = 21.2$ eV) spectra represent the total density of state (DOS), while the He II ($h\nu = 40.8$ eV) spectra represent the Cu d partial DOS, since the intensity of S and Se p contributions should be suppressed substantially at the incident photon energy of $h\nu = 40.8$ eV. Regardless of the incident photon energy, the spectra have a sharp peak about 2.7 eV below the Fermi level (E_F) for both CuS_2 and CuSe_2 , which can be assigned to the Cu t_{2g} band. The broad bands at 0–9 eV are assigned to the chalcogen p bands, because they are weak in the He II spectra. In the He II spectra, where d contribution is dominant, the broad feature at 0–2.7 eV, above the sharp t_{2g} band, represents the Cu e_g contribution, though the weak but finite p band overlaps with it. In the spectra with He I, we can clearly identify the Fermi edge for both CuS_2 and CuSe_2 , which is consistent with the fact that these compounds are metal. The fact that Fermi edge can be seen more clearly in the He I spectra than the He II spectra indicates that the chalcogen p character is dominant near E_F .

IV. DISCUSSION

A. Absence of a clear indication of strong correlation

At low temperatures, the electrical resistivity of a strongly correlated Fermi liquid is often described by $\rho = \rho_0 + AT^2$,

where ρ_0 is the residual resistivity, and the T^2 term originates from electron-electron scattering. The coefficient A is a measure of the strength of the electron-electron interaction, in proportion to the square of the specific-heat coefficient γ (the Kadowaki-Woods relationship). To check for the T^2 resistivity, $\rho - \rho_0$ versus T^2 are plotted in the inset of Fig. 2(a). As is clearly seen from the figure, the $\rho - T^2$ curve is superlinear rather than linear all the way down to 4.2 K, implying the absence of an appreciable T^2 contribution. The temperature dependence at low enough temperatures is described by $\rho = \rho_0 + B(T/\theta_{Dres})^5$, where the T^5 term is expected for electron-phonon scattering, suggesting the dominant electron-phonon contribution. Indeed, $\rho(T)$ of CuSe_2 up to room temperature can be well fitted with the Bloch-Gruneisen formula for electron-phonon-dominated resistivity. Assuming values of B are not so different between the two systems, we estimate the ratio of Debye temperatures $\theta_{Dres}(\text{CuSe}_2)/\theta_{Dres}(\text{CuS}_2) = 0.77$ by scaling the low-temperature resistivity with T/θ_D . This result is in reasonable agreement with the Debye temperatures obtained from the specific heat data shown in Fig. 3, which yield $\theta_{Dth}(\text{CuSe}_2)/\theta_{Dth}(\text{CuS}_2) = 0.60$. From these results, we conclude that electron-phonon scattering rather than electron-electron scattering dominates $\rho(T)$ of the Cu pyrites, in remarkable contrast with the other pyrites or typical correlated $3d$ transition-metal compounds.

Rather weak electron correlations are also evidenced by the density-of-state probes, namely, χ_{para} and γ . The γ values are substantially small compared with those of $\text{Ni}(\text{S,Se})_2$, which are $10\text{--}28 \text{ mJ mol}^{-1} \text{ K}^{-2}$.^{17,2} The Wilson ratio $R_W \propto \chi_{para}/\gamma$ can be a good measure of electron correlation effects. γ from the specific heat and χ_{para} from the magnetic susceptibility yield Wilson ratios of $R_W(\text{CuS}_2) = 0.76$ and $R_W(\text{CuSe}_2) = 1.09$, which suggest that these systems can be understood as weakly correlated Fermi liquids. It may be interesting to infer that R_W of a strongly correlated Fermi liquid is close to 2 in contrast to the present case. For $\text{Ni}(\text{S,Se})_2$, a value of $R_W \approx 1.6$ was obtained.² Here we note that the experimentally obtained χ_{para} and γ are about two times larger than those estimated from band calculations.^{6,10} From the facts discussed above, however, it may be difficult to take this as an enhancement due to electron correlation effects. This should be the subject of further investigation.

B. Electronic structure from photoemission study

Though transition-metal pyrites have generally been considered to be strongly correlated systems, it is now clear that copper pyrites do not show any noticeable signature of electron correlations. We believe that copper in this system is essentially monovalent (d^{10}) and nonmagnetic due to the charge transfer from the chalcogen p band, which is in remarkable contrast with the other transition-metal pyrites where the transition-metal ion is in a divalent state. Folmer *et al.* indeed suggested that copper in CuS_2 is monovalent (d^{10}), based on an analysis of core-level photoemission.^{18–20} Then holes in the anion p bands dominate the transport and magnetic properties, which reasonably accounts for the unexpected behavior of Cu pyrite.

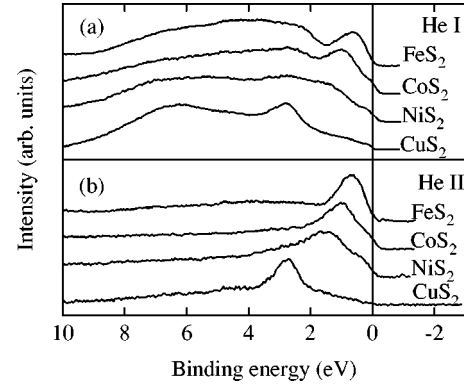


FIG. 5. Evolution of photoemission spectra of transition metal pyrites MS_2 ($M = \text{Fe, Co, Ni, or Cu}$). Here the backgrounds due to secondary electrons have been subtracted. (a) He I spectra ($h\nu = 21.2 \text{ eV}$), (b) He II spectra ($h\nu = 40.8 \text{ eV}$).

This picture is supported by the UPS spectra shown in Fig. 4. As discussed above, the reduction of intensity near E_F in the He II spectrum indicates that the d band is located well below E_F ($\sim 3 \text{ eV}$), and that the p band dominates the Fermi level. Comparison of these UPS spectra with those of the other pyrites provides further evidence of the above picture. Variations of photoemission spectra of sulfides from FeS_2 to CuS_2 are summarized in Fig. 5. The data of the other pyrites are taken from the literature.^{21–23} The sharp peaks located around $0.8\text{--}2.7 \text{ eV}$ observed both in He I and He II spectra are assigned to the metal t_{2g} band, as in CuS_2 . A well-defined shoulder structure is noticeable near E_F in the spectra from FeS_2 to NiS_2 , which can be assigned to the e_g band. It is clear that the evolution of the shoulder structure, upon going from FeS_2 to NiS_2 , represents the successive filling of the e_g band. In contrast to the other members, CuS_2 shows only a broad tail, which extends to E_F . This supports that the e_g band in Cu pyrites is indeed located at much deeper energies than the other pyrites.

The unique electronic states of the Cu pyrites may be even better illustrated by focusing on the sharp t_{2g} peak, which shifts to a higher binding energy on filling the e_g band. In CuS_2 , the t_{2g} peak position is located at a substantially higher binding energy than expected from the extrapolation based on the variation from FeS_2 to NiS_2 , which appeared to imply that there is a further stabilization of the $3d$ orbitals obtained using the d^{10} closed-shell configuration. In addition, on going from FeS_2 to NiS_2 , the t_{2g} peak shows a significant broadening. This broadening originates from its exchange splitting, as the spin polarization of the e_g band is increased with the d -band filling.²¹ If copper were divalent d^9 with three e_g electrons, the t_{2g} peak would have shown a substantial broadening. However, the t_{2g} peak in CuS_2 is as sharp as that of FeS_2 , which has no e_g electron and no spin polarization. This again proves the monovalent nature of copper in pyrites.²⁴

V. CONCLUDING REMARKS

A wide variety of experiments, including transport, magnetic susceptibility, and specific-heat measurements, revealed

that copper pyrites CuS_2 and CuSe_2 are distinct from the other metallic $3d$ transition-metal pyrites, in that the signature of strong electron correlations, such as the T^2 behavior in the resistivity, is not appreciable. This remarkable behavior originates from the monovalent (d^{10}) rather than divalent (d^9) nature of copper, and the resultant p -band character near the Fermi level. Holes are doped into the $p\pi^*$ band of the chalcogen p dimers, and dominate the transport and magnetic properties. This is experimentally proven by the UPS measurements. Copper pyrites, therefore, can be better viewed as

electron-doped molecular crystals of chalcogen dimers, namely, typical anion conductors.

ACKNOWLEDGMENTS

We thank T. Uchida for help in the synthesis. We also thank J. -Y. Son and K. Okazaki for help in the PES measurements. This work was partly supported by a Grant-in-Aid for Scientific Research, from the Ministry of Education, Culture, Sports, Science, and Technology.

- *Also at Correlated Electron Research Center, AIST Tsukuba Central 4, 1-1-1 Higashi, Tsukuba, Ibaraki 305-8562, Japan.
- ¹J. A. Wilson, *Adv. Phys.* **21**, 143 (1972).
- ²S. Miyasaka, H. Takagi, Y. Sekine, H. Takahashi, N. Mōri, and T. J. Cava, *J. Phys. Soc. Jpn.* **69**, 3166 (2000).
- ³T. A. Bither, C. T. Prewitt, J. L. Gillson, P. E. Bierstedt, R. B. Flippen, and H. S. Young, *Solid State Commun.* **4**, 533 (1966).
- ⁴R. A. Munson, W. DeSorbo, and J. S. Kouvel, *J. Chem. Phys.* **47**, 1769 (1967).
- ⁵T. A. Bither, R. J. Bouchard, W. H. Cloud, P. C. Donohue, and W. J. Siemons, *Inorg. Chem.* **7**, 2209 (1968).
- ⁶D. W. Bullett, *J. Phys. C* **15**, 6163 (1982).
- ⁷R. A. Munson, *Inorg. Chem.* **5**, 1296 (1966).
- ⁸G. Krill, P. Panissod, M. F. Lapiere, F. Gautier, C. Robert, and M. N. Eddine, *J. Phys. C* **9**, 1521 (1976).
- ⁹I. Shirovani, K. Tachi, K. Takeda, S. Todo, T. Yagi, and K. Kanoda, *Phys. Rev. B* **52**, 6197 (1995).
- ¹⁰G. Usuda and N. Hamada (private communication).
- ¹¹F. Gautier, G. Krill, P. Panissod, and C. Robert, *J. Phys. C* **7**, L170 (1974).
- ¹²*Diamagnetic susceptibility*, edited by K.-H. Hellwege and O. Madelung, Landolt-Börnstein, New Series, Group II, Vol. 16 (Springer-Verlag, Berlin, 1986).
- ¹³G. Vanderschaeve and B. Escaig, *J. Phys. (Paris) Colloq.* **37**, C4-105 (1976).
- ¹⁴G. Vanderschaeve and B. Escaig, *Mater. Res. Bull.* **11**, 483 (1976).
- ¹⁵M. Naito and S. Tanaka, *J. Phys. Soc. Jpn.* **51**, 219 (1982).
- ¹⁶J. J. Yeh and I. Lindau, *At. Data Nucl. Data Tables* **32**, 1 (1985).
- ¹⁷S. Ogawa, *J. Appl. Phys.* **50**, 2308 (1979).
- ¹⁸J. C. W. Folmer and F. Jellinek, *Less-Common Metals* **76**, 153 (1980).
- ¹⁹J. C. W. Folmer and D. K. G. de Boer, *Solid State Commun.* **38**, 1135 (1981).
- ²⁰J. C. W. Folmer, F. Jellinek, and G. H. M. Calis, *J. Solid State Chem.* **72**, 137 (1988).
- ²¹A. Fujimori, K. Mamiya, T. Mizokawa, T. Miyadai, T. Sekiguchi, H. Takahashi, N. Mōri, and S. Suga, *Phys. Rev. B* **54**, 16 329 (1996).
- ²²K. Mamiya, T. Mizokawa, A. Fujimori, H. Takahashi, N. Mōri, T. Miyadai, S. Suga, N. Chandrasekharan, S. R. Krishnakumar, and D. D. Sarma, *Physica B* **237-238**, 390 (1997).
- ²³K. Mamiya, T. Mizokawa, A. Fujimori, T. Miyadai, N. Chandrasekharan, S. R. Krishnakumar, D. D. Sarma, H. Takahashi, N. Mōri, and S. Suga, *Phys. Rev. B* **58**, 9611 (1998).
- ²⁴We analyzed the He II spectra by a standard configuration interaction calculation on the $(\text{CuS}_6)^{4-}$ cluster model. This model contains a few adjustable parameters, namely, the on-site $d-d$ Coulomb energy U , the $p-d$ charge-transfer energy Δ , and the $d-p$ transfer integrals ($pd\sigma$). We obtained $U=2.1$ eV, $\Delta=1.2$ eV, and $(pd\sigma)=1.1$ eV for CuS_2 , and $U=2.1$ eV, $\Delta=1.5$ eV, and $(pd\sigma)=0.9$ eV for CuSe_2 . These values of Δ and $(pd\sigma)$ are within the chemical trend (Ref. 25), though those of U are much smaller than expected. This discrepancy of U can be explained as the screening effect of metal, which reduce the U value. The obtained ground state consists of 60% of the d^9 state and 40% of the d^{10} state, though the cluster is supposed to consist of Cu^{2+} , namely, d^9 . In this model, only one cluster is considered though intercluster interaction is not negligible in pyrites. Though the absolute values are not reliable, this result indicates that the d^{10} state is much hybridized in the ground state. The difference of weight of the d^{10} state, between band and cluster calculations, is due to the charge of the cluster, and the difference in the high-energy excitation and low-energy excitation.
- ²⁵M. Imada, A. Fujimori, and Y. Tokura, *Rev. Mod. Phys.* **70**, 1039 (1998).